



# Studies on Backside Al-Contact Formation in Si Solar Cells: Fundamental Mechanisms

## Preprint

B. Sopori, V. Mehta, P. Rupnowski, and  
H. Moutinho  
*National Renewable Energy Laboratory*

A. Shaikh and C. Khadilkar  
*Ferro Electronic Materials*

M. Bennett and D. Carlson  
*BP Solar*

*Presented at the Materials Research Society (MRS)  
Fall Meeting 2008  
Boston, Massachusetts  
December 1-5, 2008*

**Conference Paper**  
**NREL/CP-520-45001**  
**February 2009**



## NOTICE

The submitted manuscript has been offered by an employee of the Alliance for Sustainable Energy, LLC (ASE), a contractor of the US Government under Contract No. DE-AC36-08-GO28308. Accordingly, the US Government and ASE retain a nonexclusive royalty-free license to publish or reproduce the published form of this contribution, or allow others to do so, for US Government purposes.

This report was prepared as an account of work sponsored by an agency of the United States government. Neither the United States government nor any agency thereof, nor any of their employees, makes any warranty, express or implied, or assumes any legal liability or responsibility for the accuracy, completeness, or usefulness of any information, apparatus, product, or process disclosed, or represents that its use would not infringe privately owned rights. Reference herein to any specific commercial product, process, or service by trade name, trademark, manufacturer, or otherwise does not necessarily constitute or imply its endorsement, recommendation, or favoring by the United States government or any agency thereof. The views and opinions of authors expressed herein do not necessarily state or reflect those of the United States government or any agency thereof.

Available electronically at <http://www.osti.gov/bridge>

Available for a processing fee to U.S. Department of Energy  
and its contractors, in paper, from:

U.S. Department of Energy  
Office of Scientific and Technical Information  
P.O. Box 62  
Oak Ridge, TN 37831-0062  
phone: 865.576.8401  
fax: 865.576.5728  
email: <mailto:reports@adonis.osti.gov>

Available for sale to the public, in paper, from:

U.S. Department of Commerce  
National Technical Information Service  
5285 Port Royal Road  
Springfield, VA 22161  
phone: 800.553.6847  
fax: 703.605.6900  
email: [orders@ntis.fedworld.gov](mailto:orders@ntis.fedworld.gov)  
online ordering: <http://www.ntis.gov/ordering.htm>



Printed on paper containing at least 50% wastepaper, including 20% postconsumer waste

# Studies on Backside Al-Contact Formation in Si Solar Cells: Fundamental Mechanisms

Bhushan Sopori,<sup>1</sup> Vishal Mehta,<sup>1</sup> Przemyslaw Rupnowski,<sup>1</sup> Helio Moutinho,<sup>1</sup> Aziz Shaikh,<sup>2</sup>  
Chandra Khadilkar,<sup>2</sup> Murray Bennett,<sup>3</sup> and Dave Carlson<sup>3</sup>

<sup>1</sup>National Renewable Energy Laboratory, Golden, CO 80401, USA

<sup>2</sup>Ferro Electronic Materials, Vista, CA 92083, USA

<sup>3</sup>BP Solar, Frederick, MD 21703, USA

## ABSTRACT

We have studied mechanisms of back-contact formation in screen-printed Si solar cells by a fire-through process. An optimum firing temperature profile leads to the formation of a P-Si/P<sup>+</sup>-Si/ Si-Al eutectic/agglomerated Al at the back contact of a Si solar cell. Variations in the interface properties were found to arise from Al-Si melt instabilities. Experiments were performed to study melt formation. We show that this process is strongly controlled by diffusion of Si into Al. During the ramp-up, a melt is initiated at the Si-Al interface, which subsequently expands into Al and Si. During the ramp-down, the melt freezes, which causes the doped region to grow epitaxially on Si, followed by solidification of the Si-Al eutectic. Any agglomerated (or sintered) Al particles are dispersed with Si. Implications on the performance of the cell are described.

## INTRODUCTION

The contact formation of most commercial Si solar cells is done by co-firing the cells with screen-printed front and back contacts. Typically, a gridded front-contact pattern of Ag-based ink is directly applied on the antireflection coating of SiN:H, whereas the backside has a blanket Al-based contact. The firing process, also called fire-through contact metallization, performs the following functions: (i) On the front contact, the glass frit dissolves the antireflection coating of SiN:H and allows Ag to react with Si. This reaction involves participation of a solvent metal that leaches from the glass frit and helps to lower the eutectic point of Si-Ag alloy; (ii) Diffuses hydrogen from the SiN:H-Si interface into the bulk of the cell and passivates impurities and defects; and (iii) Produces an interaction of Si and Al to form a deep back-surface field (BSF) and sinters unreacted Al to form a low-resistance contact. It is important to understand how each of these functions of this complex process can be optimized.

This paper describes our investigations on the formation of the back contact, and how most of the requirements of a good back contact can be met by a suitable process. We will first describe requirements of a back contact and then discuss our experiments and results.

### **Requirements of a Good Back Contact**

These requirements may be divided into electronic and optical categories. The electronic properties include: (i) a BSF for minority-carrier reflection, (ii) a uniform low-resistance ohmic contact, and (iii) a smooth, dimple-free surface of Al. Optically, the back contact must be reflecting with very little absorption so that it contributes effectively to light trapping. In addition to these, the process of making the back contact should be compatible with efficient gettering of impurities. In commercial solar cell fabrication, the primary consideration is given to the electronic properties, while optical reflection and gettering are assumed as byproducts,

because there is some concern whether all the requirements can be met simultaneously. Indeed, our detailed analyses indicate that the performance of the back contact of most commercial cells is below optimum.

The back-contact formation relies heavily on alloying of Si and Al to produce a controlled stratified structure. To obtain the desired electronic properties of the back contact, the kinetics of Si-Al melting and re-solidification of various phases during the firing cycle must be controlled. The next section briefly discusses requirements and issues with each region.

### **Back-surface field**

The purpose of the BSF is to provide a minority-carrier reflector that can lower the loss of photo-generated carriers at the back surface [1–6]. As is well known, the BSF arises from the band bending at the  $P^+$ -P region. Figure 1(a) illustrates the geometry of the back contact and

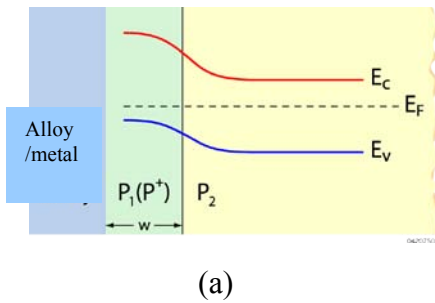
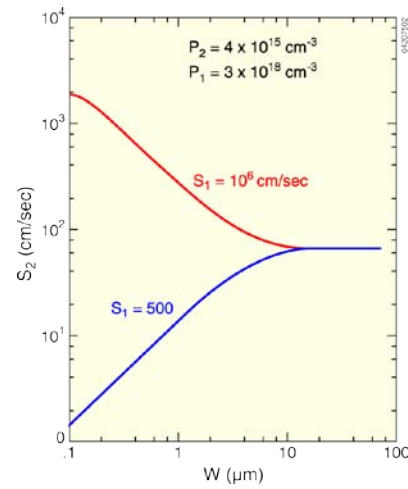


**Figure 1.** (a) Illustration of band bending within the  $P^+$ -P region, (b) calculated effective surface recombination velocity at a BSF.



shows a band diagram of the backside of a typical boron-doped solar cell. One approach to determine the effectiveness of the BSF is to determine the surface recombination velocity (SRV) of the  $P^+$ -P interface, which depends on many factors including the thickness of the  $P^+$  region. Figure 2(b) shows the calculated SRV at the back contact as a function of the thickness of the  $P^+$  region [7]. These results are given for two values of  $S_1$ . Here,  $S_1$  is the recombination velocity at the alloy- $P^+$  interface and  $S_2$  is the effective recombination velocity due to the entire contact. It is clear that the width of the  $P^+$  region should be about 10  $\mu\text{m}$  for a good BSF. Thus, it is important to determine how the cell should be processed to create a uniform, 10- $\mu\text{m}$ -wide  $P^+$  region in conjunction with a good front contact.

### **Low-resistance contact**

Low-resistance contact formation necessitates that a well-formed, ohmic contact between Si and Al be produced beyond the  $P^+$  region. An ideal contact would consist of Al/ $P^+$ /Si (as shown in Fig. 1(a)). However, as shown in the actual cross-section of a cell later in the paper, a eutectic composition accompanies the formation of the  $P^+$  region. Because the eutectic composition has a higher sheet resistivity compared to Al, this can lead to increased series resistance of the cell. An obvious way to mitigate this issue is to increase the thickness of the Si-Al eutectic. We also

show that the back contact typically leaves a region of disconnected sintered Al particles in a glass matrix. These regions can also contribute to the series resistance of the finished cell.

### **Other properties**

In addition to being a minority-carrier reflector, a back contact must also be a good optical reflector to enhance light trapping within the cell [8]. The co-firing process should also effectively getter the impurities in the cell. The details of these will be discussed elsewhere.

## **EXPERIMENT**

Experiments were done on single wafers and multicrystalline (mc) Si solar cells. These cells were fabricated on 124 mm x 124 mm, textured wafers using commercial screen-printed front and back contacts. The wafers were single crystal, single-side polished with Al deposited by electron-beam deposition either on the polished side or rough side. The firing was done in an optical furnace in which the cell is illuminated with a tailored optical flux profile, and the temperature of the wafer/cell is monitored to determine local temperatures at various critical areas such as under the metallization and away from it. All single-crystal samples were illuminated from the Si side.

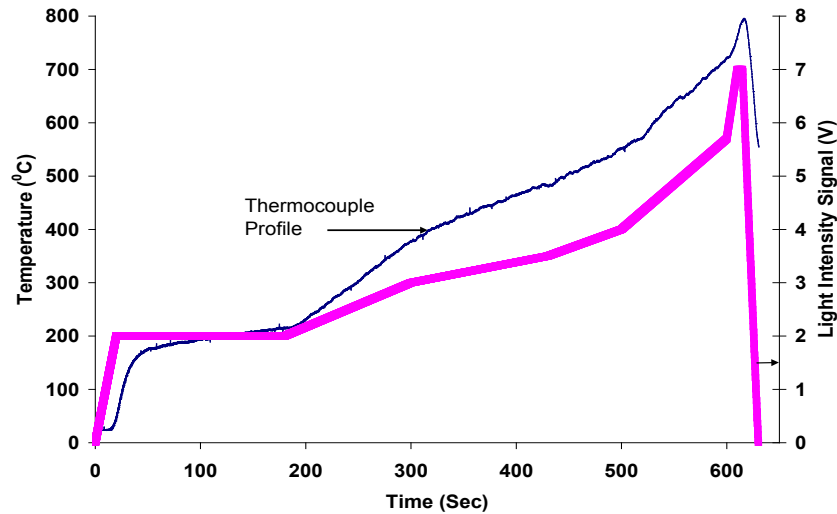


**Figure 2.** A typical firing profile along with measured cell temperature for Si solar cell.

A typical firing profile for a solar cell is shown in Fig. 2. The ramp-up segment accomplishes the following: bake the cell to drive out organics, produce a molten glass to etch the SiN:H antireflection coating, melt Si-Al on the back side, and sinter Si-Ag on the front side. The ramp-up is followed by a short constant temperature. This maximum temperature determines the maximum concentration of Al in the Si melt, which controls the maximum doping of the P+ region (see the discussion). In the ramp-down part, the molten regions of both the front and back contact solidify. Because the single-crystal samples had evaporated Al, the ramp-up portion of the profile was eliminated.

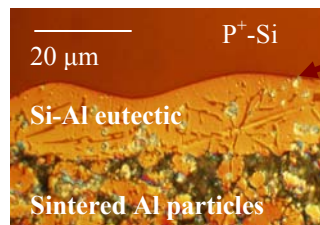
### **Characterization Techniques**

The processed samples were characterized by a variety of techniques. Scanning electron microscopy (SEM) was used for high-resolution imaging of the processed contacts and for

dopant profiling to study the BSF formation. Scanning Kelvin probe microscopy (SKPM) was used to generate potential profiles to evaluate the formation of the BSF and to determine local conductivity. Secondary-ion mass spectrometry (SIMS) profiles were used to measure Si diffusion in Al and profiles of Al after firing. Cross-sectioning was performed by a new technique [9]. This technique produces a highly flat cross-section over a large length of the cell that allows one to perform statistically meaningful analysis. Solar cells were characterized by dark and illuminated current-voltage (I-V) analyses.

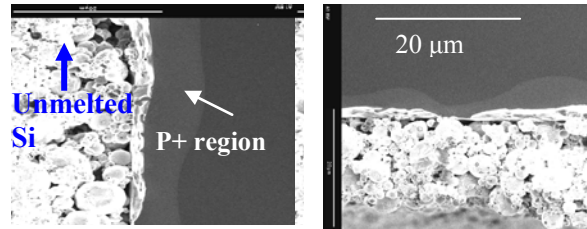
## RESULTS AND DISCUSSION

Optical microscopy of our cross-sectioned samples provided valuable information on melting of Al and formation of Si-Al alloy. Figure 3 shows an optical micrograph of the back side of an optimally fired cross-sectioned Si solar cell with screen-printed contacts. This figure shows that the back contact consists of: (i) Al-doped region that has grown epitaxially on the Si surface. The thickness of this region is about 15  $\mu\text{m}$ . The interface waviness is due to texturing of the cell. (ii) Alloyed region (Si-Al eutectic) shows typical lamellar growth consisting of Si-rich and Al-rich phases. (iii) A granular region consisting of sintered Al particles in a matrix of glass.



Interface roughness due to texturing of the wafer. Note: The texture of the interface is retained.

**Figure 3.** A cross-section of an optimally fired solar cell showing back-contact region.



(a)

(b)

**Figure 4 (a) and (b).** SEM images of different areas of same optimally fired multi-Si cell.

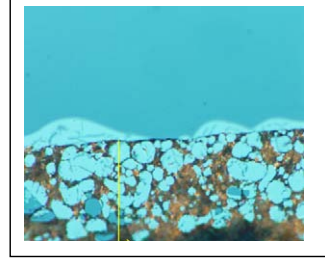
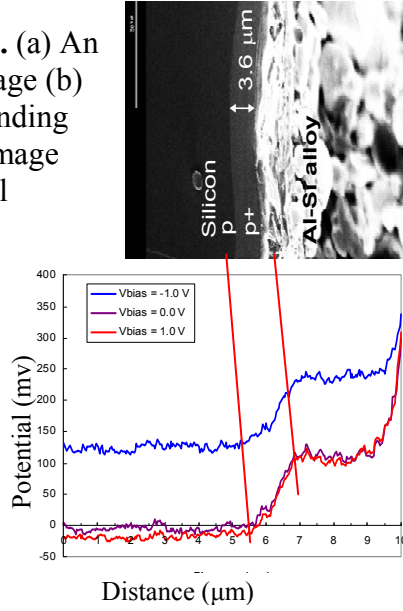
It may be noticed that some of the Al particles have melted and combined with neighboring particles. The size of the Al particle is between 5 and 20  $\mu\text{m}$ . Because our technique allows large samples to be cross-sectioned, we have observed that large variations exist in the thickness of alloyed regions and in the size of the sintered Al particles.

Figure 4 shows SEM images of the back contact of a fired mc-Si solar, taken in dopant contrast. It shows a  $\text{P}^+$  region, as well as the alloyed eutectic and sintered Al regions. The thickness of this region is only 3  $\mu\text{m}$  and varies along the length of the interface. Figure 4b is an image of another section of the same cell showing a significant variation in the thickness of the alloyed layer and of  $\text{P}^+$  region and that some correlation exists between the thicknesses of these regions.

Figure 5a shows an SEM image of a back contact and its potential profile (Fig 5b) under different bias conditions obtained by SKPM. A voltage of 110 mV appears across this  $\text{P}^+$ - $\text{P}$  region. Figure 6 is an optical micrograph showing a very important feature of the alloy thickness variation; the thickness of the alloy is largest at the valley of the texture and a minimum at the peak of the texture. This indicates that during the formation of Si-Al alloy, the melt initially fills up the texture valley. Any excess melt spills over the adjacent valleys and then builds up. The depth of the  $\text{P}^+$  region is generally larger at thicker alloyed regions.



**Figure 5.** (a) An SEM image (b) corresponding SKPM image (potential profile).



**Figure 6.** Optical micrograph of a c/s cell, showing thickness variations of the alloyed region corresponding to the textured profile of the Si.

Our results show that the melting and solidification of the back Al contact agrees well with the binary phase diagram of Al and Si [10]. It is rather remarkable that the general (qualitative) features of the phase diagram, which is applicable to a thermal equilibrium process, are indicated in our results (which may not be an equilibrium process). Indeed, there are variations imposed by the departures from a phase diagram. These departures arise from the following:

1. We have observed that the firing process involves a very rapid diffusion of Si into Al. This diffusion controls the initial composition and location of the initial melt near the Si-Al interface. Figure 7 shows a SIMS profile of Si diffused into Al caused by a short firing profile; the thickness of Al was kept at only 1 micron to show that the diffused Si can accumulate at the Al-air interface. In a screen-printed cell, the diffused Si can disperse between melted Al particles. Figure 8 shows an SEM (Fig. 8a) and EDX images of Si (Fig 8b) and Al (Fig 8c). In Fig. 8b, one can see that Si has diffused deep into Al beyond the alloyed region. The presence of Si around Al particles will cause an increase in the series resistance of the cell.
2. Melting of Al on a Si surface produces a very nonuniform melt because of high surface tension (large contact angle) and balling up into Al spheres. This phenomenon will lead to pockets of melt of different sizes, concomitantly producing  $P^+$  and Si-Al eutectic regions of different thicknesses (as seen in Figs. 4 and 6). We have found that Si diffusion into Al can be used to increase the adhesion between the Al melt and Si, thereby producing a uniform melt, and hence, a uniform contact.
3. During ramp-down, the melt cools and tries to regrow epitaxially over Si. This doped layer of Si follows the topology of the Si surface. On further cooling, an outside layer of Al freezes, which traps a liquid layer between solid Al (particles) and Si (with regions of soft glass). As the melt reaches the eutectic point, the entire melt is expected to freeze. It may be recognized that beyond the eutectic point Si will continue to diffuse into Al-Si and will pile up at interstitial spaces. Another important significance of diffusion of Si is that it competes with Al for oxygen that may be available at the interface, and it prevents a strong oxidation of melted Al particles to allow them to join with each other.

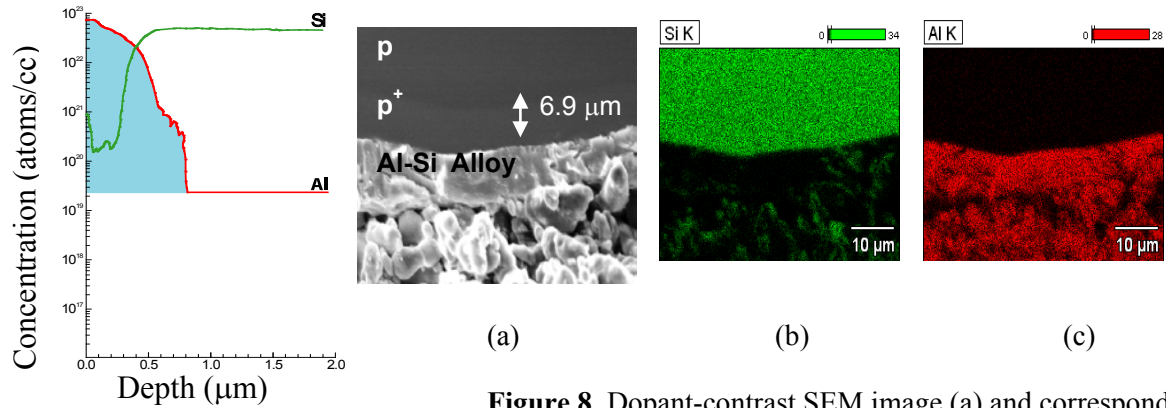


**Figure 7.** SIMS profile of Si diffusion in Al.

**Figure 8.** Dopant-contrast SEM image (a) and corresponding EDX images of (b) Si and (c) Al.

## CONCLUSION

An optimum firing temperature profile leads to the formation of a P-Si/P<sup>+</sup>-Si/ Si-Al eutectic/unmelted Al at the back contact of a Si solar cell. Variations in the interface properties were found to arise from Al-Si melt instabilities. Experiments show that melt formation is strongly controlled by diffusion of Si into Al. This affects the series resistance of the cell.

Based on the above results, a desirable profile should encourage initial Si diffusion. This will initiate a melt very close to the eutectic point of 577°C. Next, the temperature should be raised to about 775°–800°C to ensure an adequate amount of Al concentration in the melt to form heavily doped P<sup>+</sup> upon solidification. The duration of the peak temperature strongly controls the total thickness of P<sup>+</sup> and the eutectic regions. However, a slow cooling from peak temperature to the eutectic point is desirable to ensure a large P<sup>+</sup> region.

## REFERENCES

1. J. D. Alamo, J. Eguren, and A. Luque, *Solid-State Electron.* **24**, 415 (1981).
2. C. Khadilkar, S. Kim, A. Shaikh, S. Sridharan, and T. Pham, *Tech. Digest. of International PVSEC- 15*, (2005).
3. A. Kaminski, B. Vandelle, A. Fave, J.P. Boyeaux, L. Q. Nam, R. Monna, D. Sarti, and A. Laugier, *Solar Energy Materials & Solar Cells* **72**,373 (2002).
4. S. Narasimha, A. Rohatgi, and A. W. Weeber, *IEEE Trans. on Electron Devices* **46**(7), 1363 (1999).
5. F. Huster and G. Schubert, 20<sup>th</sup> European Photovoltaic Solar Energy Conference and Exhibition, Barcelona, 2DV2.48, 6–10 June (2005).
6. C.H. Lin, S. Y. Tsai, S. P. Hsu, and M. H. Hsieh, *Solar Energy Materials & Solar Cells* **92**, 986 (2008).
7. B. Sopori, V. R. Mehta, P. Rupnowski, D. Domine, M. Romero, H. Moutinho, B. To, R. Reedy, M. Al-Jassim, A Shaikh, N. Merchant, and C. Khadilkar, Proc. 22<sup>nd</sup> European Photovoltaic Solar Energy Conference, Milan, 841(2007).
8. M. Cudzinovic and B. Sopori, Proc. 25<sup>th</sup> IEEE PVSC, 501 (1996).
9. B. Sopori, V. Mehta, N. Fast, H. Moutinho, D. Domine, B. To, and M. Al-Jassim, Proc. 17<sup>th</sup> Workshop on Crystalline Silicon Solar Cells & Modules: Materials and Processes, Vail, Colorado, 222 (2007).
10. J. L. Murray and A. J. McAlister, *Bull. Alloy Phase Diagrams* **5**, 74 (1984).



**REPORT DOCUMENTATION PAGE**Form Approved  
OMB No. 0704-0188

The public reporting burden for this collection of information is estimated to average 1 hour per response, including the time for reviewing instructions, searching existing data sources, gathering and maintaining the data needed, and completing and reviewing the collection of information. Send comments regarding this burden estimate or any other aspect of this collection of information, including suggestions for reducing the burden, to Department of Defense, Executive Services and Communications Directorate (0704-0188). Respondents should be aware that notwithstanding any other provision of law, no person shall be subject to any penalty for failing to comply with a collection of information if it does not display a currently valid OMB control number.

**PLEASE DO NOT RETURN YOUR FORM TO THE ABOVE ORGANIZATION.**

<b>1. REPORT DATE (DD-MM-YYYY)</b> February 2009			<b>2. REPORT TYPE</b> Conference Paper		<b>3. DATES COVERED (From - To)</b> December 1-5, 2008	
<b>4. TITLE AND SUBTITLE</b> Studies on Backside Al-Contact Formation in Si Solar Cells: Fundamental Mechanisms; Preprint					<b>5a. CONTRACT NUMBER</b> DE-AC36-08-GO28308	
					<b>5b. GRANT NUMBER</b>	
					<b>5c. PROGRAM ELEMENT NUMBER</b>	
<b>6. AUTHOR(S)</b> B. Sopori, V. Mehta, P. Rupnowski, H. Moutinho, A. Shaikh, C. Khadilkar, M. Bennett, and D. Carlson					<b>5d. PROJECT NUMBER</b> NREL/CP-520-45001	
					<b>5e. TASK NUMBER</b> PVA93110	
					<b>5f. WORK UNIT NUMBER</b>	
<b>7. PERFORMING ORGANIZATION NAME(S) AND ADDRESS(ES)</b> National Renewable Energy Laboratory 1617 Cole Blvd. Golden, CO 80401-3393					<b>8. PERFORMING ORGANIZATION REPORT NUMBER</b> NREL/CP-520-45001	
<b>9. SPONSORING/MONITORING AGENCY NAME(S) AND ADDRESS(ES)</b>					<b>10. SPONSOR/MONITOR'S ACRONYM(S)</b> NREL	
					<b>11. SPONSORING/MONITORING AGENCY REPORT NUMBER</b>	
<b>12. DISTRIBUTION AVAILABILITY STATEMENT</b> National Technical Information Service U.S. Department of Commerce 5285 Port Royal Road Springfield, VA 22161						
<b>13. SUPPLEMENTARY NOTES</b>						
<b>14. ABSTRACT (Maximum 200 Words)</b> We have studied mechanisms of back-contact formation in screen-printed Si solar cells by a fire-through process. An optimum firing temperature profile leads to the formation of a P-Si/P+-Si/ Si-Al eutectic/agglomerated Al at the back contact of a Si solar cell. Variations in the interface properties were found to arise from Al-Si melt instabilities. Experiments were performed to study melt formation. We show that this process is strongly controlled by diffusion of Si into Al. During the ramp-up, a melt is initiated at the Si-Al interface, which subsequently expands into Al and Si. During the ramp-down, the melt freezes, which causes the doped region to grow epitaxially on Si, followed by solidification of the Si-Al eutectic. Any agglomerated (or sintered) Al particles are dispersed with Si. Implications on the performance of the cell are described.						
<b>15. SUBJECT TERMS</b> PV; back-contact formation; solar cells; fundamental mechanisms; impurities;						
<b>16. SECURITY CLASSIFICATION OF:</b>			<b>17. LIMITATION OF ABSTRACT</b> UL	<b>18. NUMBER OF PAGES</b>	<b>19a. NAME OF RESPONSIBLE PERSON</b>	
<b>a. REPORT</b> Unclassified	<b>b. ABSTRACT</b> Unclassified	<b>c. THIS PAGE</b> Unclassified			<b>19b. TELEPHONE NUMBER (Include area code)</b>	

Standard Form 298 (Rev. 8/98)  
Prescribed by ANSI Std. Z39.18